ARTICLE

Corrosion Control of Coated Structural Components in Marine Environment

G. L. Manjunath[1]   S. Surendran[2]*

1. Department of Ocean Engineering, Indian Institute of Technology Madras, Chennai, India
2. Department of Ocean Engineering, Indian Institute of Technology Madras, Chennai, India

ARTICLE INFO	ABSTRACT
	Tropical waters are with more salinity and harbor millions of micro organisms. Such environmental condition challenges the strength and reliability of marine structures. The behaviour of structural materials due to pitting and uniform corrosion is studied, and a method based on coating is suggested to improve the life cycle ensuring reliability in its functionality. The structural materials like high strength steel and AA6063 were selected for the study and metallic coating performed for evaluation of corrosion resistances. Samples are investigated in chloride concentration of 3.5% NaCl by weight loss measurements and potentiodynamic polarization. The coating was done by electroplating and PVD (Physical Vapour Deposition) method for high strength steel, where as aluminum samples were coated by an electroplating method. The high strength steel samples were mono coated by Ni and Cr using the electroplating method, and composite coating was done with Al-N (Aluminium nitride) and Ti-Al-N (Titanium Aluminium Nitride) by PVD techniques. Scanning electron microscopy (SEM) was used for evaluation of fracture toughness of coating around the pits formed. The investigation showed that the methods and thickness of coating influenced corrosion resistances of the substrate metals. Composite coated samples by PVD showed excellent corrosion resistance properties compared to electroplated samples after the investigations. Finite element analysis was performed by FRANC 2D/L (Fracture Analysis Code) showed a decrease in stress intensity values for composite coated samples of PVD compared to mono coated electroplated samples. Increase in the duty cycle of the structure was observed in the simulation has a result of a decrease in stress intensity values for PVD coated samples.

1. Introduction

The reliability and serviceability of marine structures are always challenged in the marine environment due to corrosion. Corrosion degrades the performance of the structural components for different loading conditions. The corrosion induces fatigue due to variable loadings is another challenge to the designer as this leads to premature aging of structures. And aging may lead to the growth of single and multiple cracks with different types of loading. As the metal corrodes the crack tip may get blunt which may lead to sudden failure or branching of cracks and the repair of these types of

Corresponding Author:

S. Surendran

Department of Ocean Engineering, Indian Institute of Technology Madras, Chennai, India

Email: sur@iitm.ac.in

failures becomes difficult. The effective performance of structural components in the severe marine environment is a matter of concern and corrosion as become a major area of study. Petroyiannis et al.[1] focused on the mechanical behavior of corroded aircraft components AA2024 by conducting experiments. A moderate reduction in yield, ultimate tensile stress, and strain energy density are observed due to a reduction in thickness. Reduction in mechanical properties does not affect the tensile ductility, and experiments suggest that corrosion is due to hydrogen embrittlement. Some researchers developed a mathematical model for explaining the multi-scaling concepts like fracture toughness, residual strength, and strain energy density. Pantelakis et al.[2] evaluated the corrosion susceptibility of aluminum alloys used in aircraft structures and calculated tensile and energy density data. Samples were pre-corroded by accelerating corrosion tests and found a decrease in yield and ultimate tensile stress. Authors found that hydrogen penetration and absorption was the main reason for material degradation and volumetric embrittlement. Birchon [3] briefly reviewed on the selecting nature of materials and fabrication processes on the performance of structures in ocean engineering. The author also emphasized the material weakness and capabilities in offshore, due to corrosion induced fracture and fatigue.

Harlow and Wei [4] discussed the effects of pitting corrosion and its effects on the durability and integrity of structures. Authors studied the rate of pit growth and proposed some probability models for the growth of corrosion pits in aluminum alloys in aqueous environments. Statistically estimated the size of the corrosion pits at a given time for multi-site damage and cracked growth by proposing a mathematical model. Pidaparti and Rao[5] investigated the corrosion damage in structural components like aluminum and steels used for aerospace and naval structural applications. Authors used CAD (Computer Aided Design) for modeling the pits and FEM (Finite Element Method) for predicting the stresses in single and multiple pits. The analysis was done for estimating stress distributions on the corroded surface as a function of time and sample surface layers. Authors observed the formation of micro cracks around the main pitted area this lead to nucleation and coalescence of fine cracks and finally resulted in differential stresses along the sample thickness. Gooch and Booth [6] paid attention to the aspects of offshore design and corrosion fatigue of steel structures. Authors studied the variable effects like cyclic stress conditions, environmental factors, and material characteristics and their influence on structural response. Lynch [7] studied some cases of failures and generalized the procedures to analyze failures. They suggested a procedure to over-

come the shortcomings due to stress cracking. Corrosion fatigue, hydrogen embrittlement and liquid-metal embrittlement in aluminium alloys, high-strength steels etc, . were the topic of interest to the author. Moan, and Uraga [8] addressed ship hull maintenance under combined crack growth, corrosion on structural components by proposing a reliability-based model. Reliability model takes into account of corrosion-induced crack growth rate in two ways increase in stress range by the plate thinning and corrosion induced fatigue. Sensitivity studies and hazard rate concept were adopted with different case studies by inspecting the hulls at regular interval of time. Dale et al. [9] demonstrated the corrosion damage assessment framework for aging aircraft structures they evaluated several tools like FRANC2D/L for stress distribution, AFGROW for fatigue crack growth and PROF for the probability of fracture. The structural analysis was done for crevice corrosion and multiple site damage in fuselage lap joints and compared with experimental results and showed a good agreement in the interesting parameters.

Gangloff [11] discussed modern laboratory testing techniques for corrosion fatigue and their principles and mechanisms involved. Emphasis was given to specimen design, loading, environmental controls, strain and crack size measurements later on data analysis and interpretation. The author showed the complexities associated with the corrosion fatigue effects in the performance of structural metals. Zaid et al. [16] studied the corrosion behavior of AA6061 alloy considering the effect of pH and chloride concentration of NaCl solution by weight loss measurement tests, potentiodynamic polarisation, linear polarization, and cyclic polarisation followed by SEM analysis. Authors found that pH and chloride concentration of NaCl solution affected the corrosion behavior of AA6061 alloy. Hemispherical and cryptographic pits were formed as a result of localized corrosion. Tamura et al. [17] concentrated on models for explaining corrosion reactions. This included the formation of rust and pH effect on the corrosion rate. Authors paid attention to the rust films stoppage and passage of anions by deteriorated rust film separation of cathode and anode leading to crevice corrosion. Pidaparti et al.[18] suggested nondestructive testing techniques for structural health maintenance of structure using image analysis for studying the corrosion morphology by wavelet transformation and fractals useful for correlating service and failure conditions. Authors studied on pits formation and initiation and growing cyclically leading to material failures based on corrosion conditions and applied stress. Allachi et al.[19] studied the uniform and pitting corrosion processes on AA6060 alloy in the presence of small concentrations of cerium chloride to

3.5% NaCl. Authors mainly focussed on the determination of the protection and inhibition character of cerium ion by SEM and EDS spectra. Park[20] studied the structural integrity of aging ships by focussing the study on corrosion, fatigue cracking and formation of local dents developed during the time of ship service. The risk assessments of the ships were aimed by studying the ultimate strength characteristics of the ship structure. Paik and Kim[21] developed a corrosion wastage model by understanding the phenomenon of aging of the ballast tank structures. The proposed model was able to predict the time-dependent corrosion wastage accurately. The study was helpful in judging the performance of the ship in the marine environment and periodical inspection with the ship structures for safe operations. Mohd Hairil Mohd et al.[22] used magnetic flux leakage tool for as a nondestructive evaluation (NDE) technique for evaluating the corrosion depth and width in gas pipelines. The NDE techniques help in accurate predictions of the reliability of the aged structures. Authors developed some time-dependent corrosion models for estimating pitting corrosion depths by undergoing statistical studies. The proposed model predicted the pit depth at any given age just by changing scale, shape and location parameters. The above inputs help in designing a new gas pipeline saves a huge amount of risks, economy and time. Manjunath and Surendran [23] metallically coated samples were exposed to different temperatures and corrosive environment, and a difference in dynamic fracture toughness values was noted. The method of coating influenced the performance of the substrate metals.

Currently, in the present work, high strength steel and AA6063 samples were coated with two different methods of coating like electroplating and PVD (physical vapor deposition). The high strength steel samples were electroplated by Ni (nickel) and Cr (chromium) in steps of 6µ, 20µ, 40µ, and 60µ whereas PVD samples coated with a 6µ thickness only because of limitations. Aluminum samples were coated with Ni in steps of 6µ, 20µ, 40µ and 60µ. Samples were tested by potentiodynamic polarization. The samples which were coated with PVD showed excellent corrosion resistance in the case of potentiodynamic polarization and uniform corrosion. Later thinning effects were considered in the finite element analysis done using FRANC 2D/L. The fatigue crack growth life cycle of coated and uncoated samples was estimated before and after corrosion and compared.

2. Experimental & Simulation Details

Two types of testing were carried out in the present work, potentiodynamic tests for pitting corrosion and weight loss test for uniform corrosion. The required sample dimension for the potentiodynamic test is the 25.4mm diameter and 10mm thickness, and for uniform corrosion, it is 55mm length, 10mm width, and 10mm thickness. A V notch at the center of 2mm depth was considered. Samples are coated by PVD and electroplating for steel samples and in aluminum only electroplating is done. Steel samples were coated with Ni and Cr in electroplating and PVD composite coating of Al-N, and nano crystalline material of Ti-Al-N was done, for AA6063 alloys electroplating of Ni was done. The coating thickness was in the steps of 6µ, 20µ, 40µ and 60µ in electroplating. Only 6µ coating thickness was done using the PVD method.

Potentiodynamic polarization was done for all the samples of steel and aluminium and a corresponding graph of E (voltage) v/s I (current density) was obtained for each sample. Corresponding E_{corr} and I_{corr} values are obtained for each sample by drawing the tangents for anode and cathode curves, pitting corrosion rate for each sample was obtained. The steel samples were tested in 3.5% NaCl solution, and in case of aluminum samples were tested in 3.5% NaCl, and NaOH added to maintain the pH value while conducting the experiment (buffering the solution). For uniform corrosion, a weight loss test was performed for 2400 hours the weight of the samples were noted for calculating corrosion rate. The uncoated and coated samples of steel and aluminum samples were soaked in 3.5% NaCl with a pH value of 7.

Figure 1. (a) Electro chemical set up

Figure 1. (b) Sample along with cell components

Figure 1. (c) Samples corroded in 3.5% NaCl

Figure 1. (d) Samples after corroding for 2400 hours

Figure 1. (e) 6μ Coated samples of PVD and electroplated samples corroded for 2400 hours

Figure 1. (f) 20μ Samples of Ni and Cr corroded for 2400 hours.

Figure 1. (g) from left to right: uncoated sample of aluminum, 6μ Ni coated aluminum, 20μ Ni coated aluminum, 40μ Ni coated aluminum and 60μ Ni coated aluminum after corroding for 2400 hours

The figures 1 (a) and 1 (b) shows the cell set up along with arrangements for potentiodynamic polarization. In figures 1 (c) and 1 (d) the samples are corroded in 3.5% NaCl for 2400 hours and washed with distilled water thoroughly before seeing the weight of the corroded samples. Figure 1(e) showed how the sample is being corroded near notch and compared to other electroplated samples (on the right side) the PVD coated samples (to the left showed) more corrosion resistance. The 20μ electroplated samples of Cr sample to the right were better corrosion resistance compared to Ni samples to the left. Aluminum samples showed the phenomenon of deposition of salt on the surface. The salt is getting deposited on the surface of 6μ Ni coated aluminum samples. The removal of deposited salt from the surface can result in removal of the substrate. Comparatively, the coated samples are corroding fast compared to uncoated samples.

ASTM G-59 proposed standard test method for conducting potentiodynamic polarization resistance measurements [13]

$$\text{Corrosion Rate} = \left[\frac{3.27 \times 10^{-3} \times i_{corr} \times EW}{\text{Density}} \right] \quad (1)$$

Where corrosion rate is measured in mmpy, icorr is corrosion current density; EW is the equivalent weight of corroding samples, an area in mm^2 and density in g/cm^3.

Equation for uniform corrosion rate as per [14]

$$\text{Corrosion Rate} = \left[\frac{1000 \times \text{Weightloss} \times 365}{\text{Time} \times \text{Area} \times \text{Density}} \right] \quad (2)$$

Where corrosion rate is measured in mmpy, weight loss in grams, time in days, an area in mm^2 and density in g/cm^3.

Effective stress intensity factor Keffective is calculated for different crack lengths taken from [12]

$$K_{effective} = \sqrt{K_I^2 + \beta K_{II}^2} \qquad (3)$$

Where K_I and K_{II} are used to denote fractures in mode I and mode II and β co-efficient is the material characteristic [15]

$$K_{Ic} = 0.0319 \frac{P}{a\sqrt{c}} \qquad (4)$$

Equation (4) is used for evaluating the fracture toughness of coating much thicker than 1μ, the fracture toughness K_{Ic} depends on applied load P and indenter size at which causing a crack c in the coating. The indentation is done by Vickers micro hardness tester on the coating before and after corroding. In pitting corrosion around the pits, the indentation was done to evaluate coating toughness around the pits later it was done for uniformly corroded sample near the notch area which was found to be weak. The pitting and thinning effects from the experiment are considered, and simulation is carried out in FRANC 2D/L. Uniform and pitting corrosion are considered individually for the different duration in some years, later the uniform and pitting are included together, and analysis was carried out. The analysis was performed for multiple cracks, and those with high $K_{effective}$ was considered for the study. Corresponding $K_{effective}$ (effective stress intensity factor) values in mode I and II is calculated differently for crack length. Fatigue crack growth simulation after the corrosion was done for multiple cracks and the crack which is showing the least number of cycles is taken.

3. Results and Discussion

The uniform and pitting corrosion tests were conducted to study the corrosion effect on crack growth due to cyclic loading responsible for the catastrophic failure of the structure. In pitting growth, a pit can cause the growth of other micro pits around it leading to multiple cracks. The phenomenon of multiple cracking is assumed in uniformly and pitting corroded samples individually due to corrosion. Both uniform and pitting corrosion is considered together for samples by assuming uniform corrosion to occur first followed by pit formation. To overcome the above problems a technique of coating is adopted in the present work; coating helps to reduce the corrosion rate thus enhancing the life of the structure. Selection of coating material depends on adhesive strength and depends on the ability towards corrosion. The permeability in coating decides the durability and transition temperature of the coating. Potentiodynamic tests on electroplated Ni aluminum samples showed the increase in corrosion resistance with an increase in coating thickness as per figure 2. The coated and uncoated samples of aluminum were tested

in 3.5% NaCl, and NaOH added to maintain the pH. The formation of pits can be seen in almost every coated and uncoated samples of aluminum.
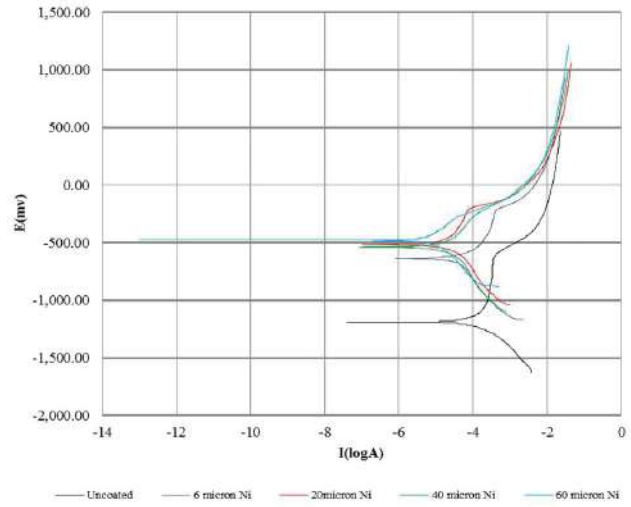

Figure 2. E_{corr} Vs. I_{corr} for coated and uncoated aluminum samples

The potentiodynamic polarization of electroplated steel samples showed an increase in corrosion resistance with an increase in coating thickness. Electroplated Ni samples of steel showed the formation of pits in all the coated samples with coating thickness varying from 6μ, 20μ, 40μ and 60μ shown in figure 3. In Cr electroplated samples of steel, pits are observed in 6μ, 20μ and 40μ samples except in 60μ case. When the PVD coated samples were tested, the 6μ Al-N steel coated sample showed a slight wearing out of the surface due to corrosion, and in 6μ Ti-Al-N no such phenomena were seen thus was a case of excellent corrosion resistance.
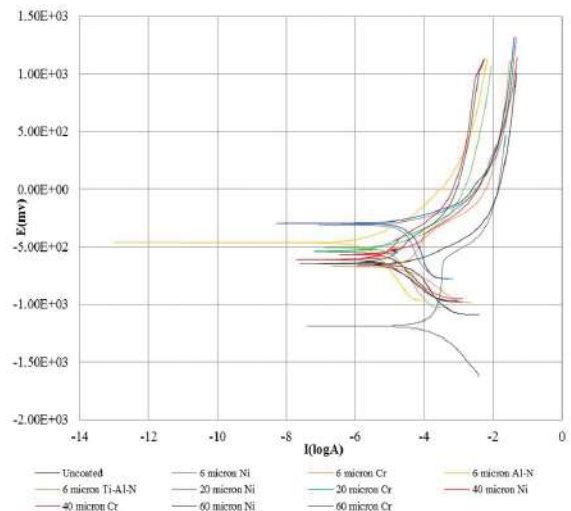

Figure 3. E_{corr} Vs. I_{corr} for coated and uncoated steel samples

After the weight loss experiment, the corrosion rate against corrosion time was plotted for uniform corrosion of both coated and uncoated samples. Parent metals of steel and aluminum were considered, and equation two was relied upon. In the case of Ni and Cr electroplated steel samples the increase in coating thickness reduced the corrosion rate and in PVD coated Al-N and nano crystalline Ti-Al-N steel samples was found to be still shown in figure 4. In Ni electroplated sample of aluminum the salt started to deposit on the 6μ Ni coated samples. No salt deposition was observed in uncoated samples of aluminum. Removing the deposition of salt from samples in 6μ Ni coated samples resulted in the removal of substrate material. For aluminum this is equivalent to an increase of corrosion rate.
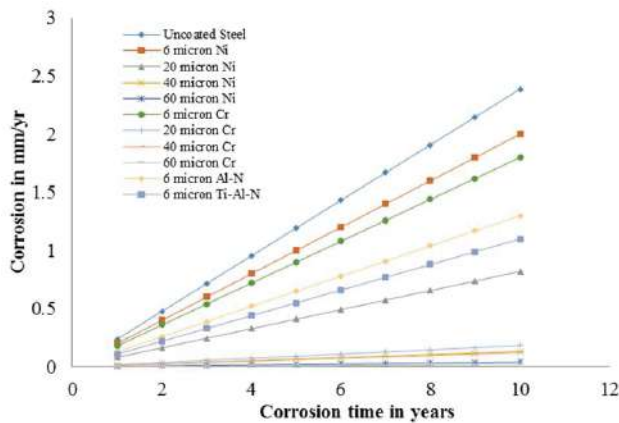
Figure 4. corrosion rates against corrosion time for uniformly corroded steel samples
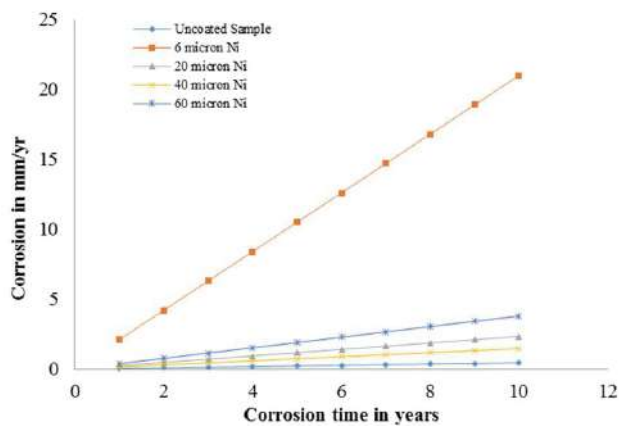
Figure 5. Corrosion rates against corrosion time for uniformly corroded aluminum samples

As per the potentiodynamic polarization, the pitting corrosion rate against time is reduced due to an increase in coating thickness. For coated and uncoated steel and aluminum samples a comparison of figure 6 and seven will easily convince this.
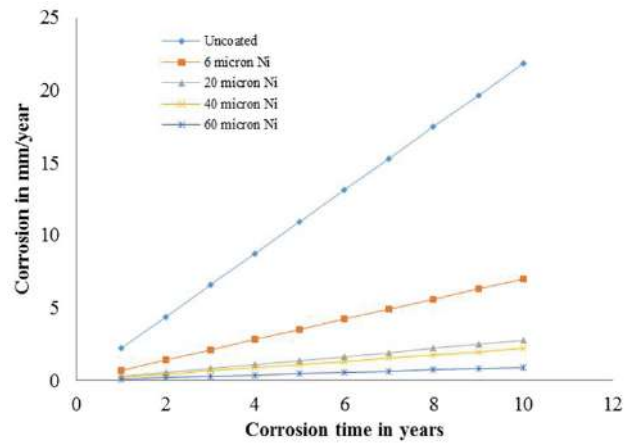
Figure 6. Corrosion rates against corrosion time for pitting corroded aluminum samples
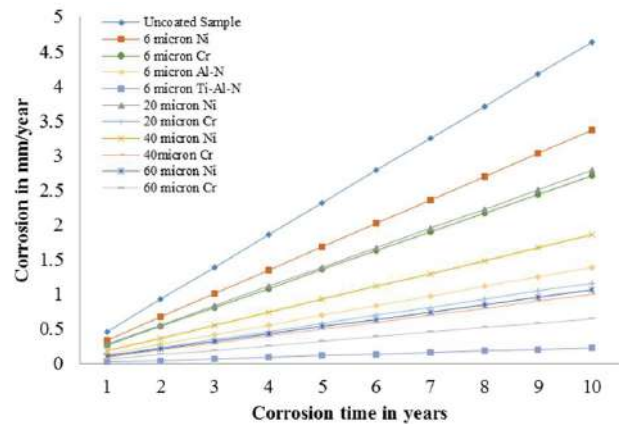
Figure 7. Corrosion rates against corrosion time for pitting corroded steel samples

Different combinations of corrosion rates, pitting and uniform corrosion are considered by deducting the thickness from the sample. The increase in thickness shows an increase in corrosion rate and reduced performance of the structural components. The corrosion rate against corrosion time is plotted considering the combination is shown in figure 8 and figure 9 for steel and aluminum. The steel samples showed an increase in corrosion rate compared to aluminum shown in figure 8 and 9. The influence of coating thickness on corrosion is proved here, through not directly. Classification societies insist on the renewal of plates, stiffness and structural part based on the diminishing of thickness on a percentage basis. It varies from location to location on ship hull contour.

Tropical waters deteriorate the hull structure more rapidly compared to the Arctic, North Atlantic waters, etc. Hull designers will more be interested in the mechanical strength properties of steel and aluminum after getting corroded. Next part deals with the variation in fracture
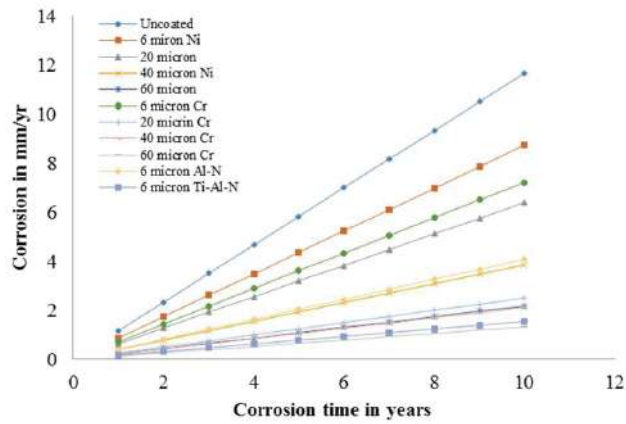
Figure 8. Corrosion rates against corrosion time for pitting and uniformly corroded steel samples
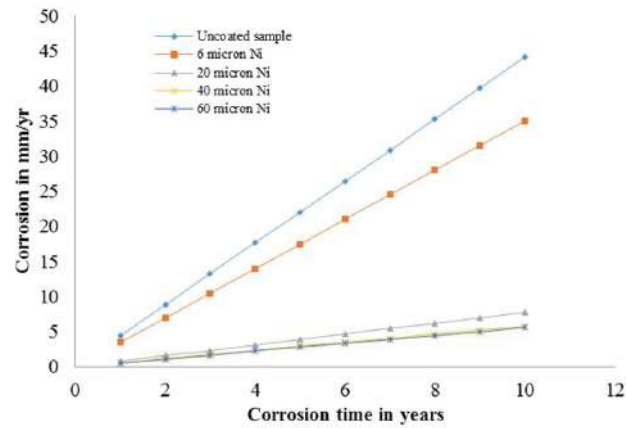

Figure 9. Corrosion rates against corrosion time for pitting and uniformly corroded aluminum samples

toughness due to the diminishing of thickness due to corrosion. The simulation was done by FRANC 2D/L, and the corresponding $K_{effective}$ against crack lengths were calculated for uniform and pitting corrosion initially, and later both were combined. $K_{effective}$ against crack lengths is calculated for 1 and five years respectively for coated and uncoated samples of steel and aluminum. $K_{effective}$ values found increasing with increase in corrosion time for uncoated samples. Coated steel samples showed a decrease in $K_{effective}$ with an increase in coating thickness in case of an electroplated sample of steel from figures 11 and 12. In figures 11 the value of $K_{effective}$ is found less compared to figures 12 in which the $K_{effective}$ is found increasing due to increasing in corrosion rate. The Al-N and Ti-Al-N samples showed corrosion resistance with coating not getting peeled off near the notch, while in electroplated samples peeling of coating near the notch can be observed in case of steel samples. Multiple cracks were grown near the uniformly corroded area and crack with high $K_{effective}$ was

considered for the analysis. The reduction in thickness of sample will affect the $K_{effective}$ values and even cause a grouping of cracks.
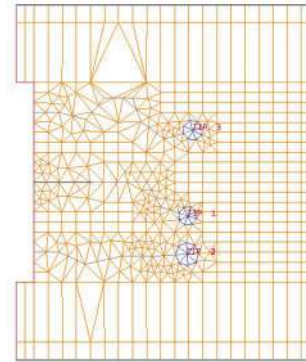
Figure 10. Crack growth for uniformly corroded samples
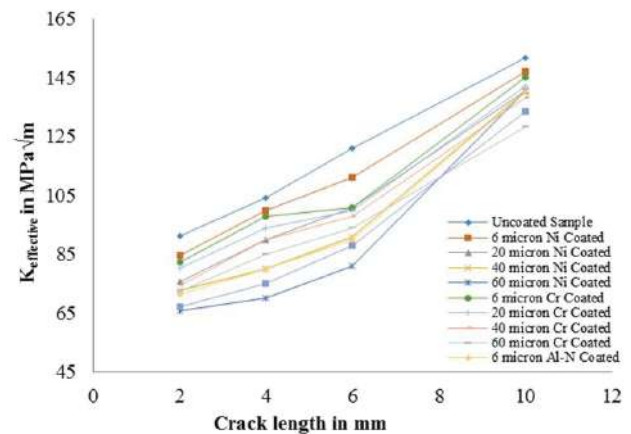
Figure 11. $K_{effective}$ against crack length for one year uniformly corroded steel samples
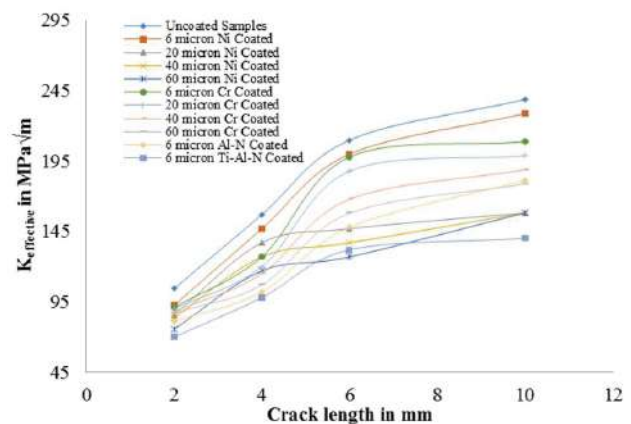
Figure 12. $K_{effective}$ against crack length for five year uniformly corroded aluminum samples

Figure 12 clearly explains that the increase in coating increased the corrosion resistance and indirectly reduced the $K_{effective}$ values. Particularly the 60μ coated samples

27

and 6μ PVD coated samples showed almost linear variations. But in the case of other uncoated and electroplated samples, a nonlinear behavior can be observed in 6μ, 20μ and 40μ samples from figure 12. The 6 Cr coated case is showing a higher order nonlinearity of stress intensity factor. The above corrosion calculations are considered in the simulation, and different cracks are grown at different regions as per figure 13. The occurrence of the first crack can influence the behavior of the other two cracks. Figure 13 also illustrates that the crack may either cut each other or the stress radiated from one crack can cause the deflection of the nearby crack.
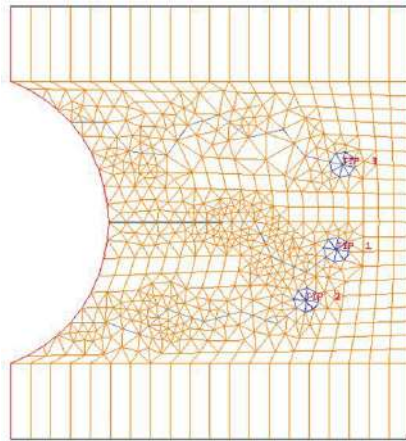
Figure 13. Crack growth for pitting corroded samples

The pitting corrosion results showed a decrease in $K_{effective}$ for PVD coated samples compared to electroplated samples. In pitting the $K_{effective}$ is found high compared to uniform corroded samples because of stress concentration at the pits formed. The pits formed can cause the growth of one or more cracks which may grow under the cyclic loading and corrosive environment in order to simulate this condition, multiple cracks as assumed near the pits to study the influence of pits and crack with high $K_{effective}$. Figure 14 shows a highly nonlinear behavior for uncoated and 60μ Ni electroplated samples compared to other examples the trend of which are almost linear. The increase coating thickness may lead to peeling off coating in electroplated samples.

In figure 15 an increase in the corrosion rate influenced the crack kinking and hence more $K_{effective}$ values. More importantly with an increase in crack length at around 6mm a severe shift in the values of $K_{effective}$ can be observed. The PVD coated samples and those with higher coating thickness showed a linear variation after a crack length of 6mm. As expected a lesser value of $K_{effective}$ are seen in figure 15. It can be inferred that the method of coating effects the adherence properties of the substrates and influences the corrosion resistance properties.
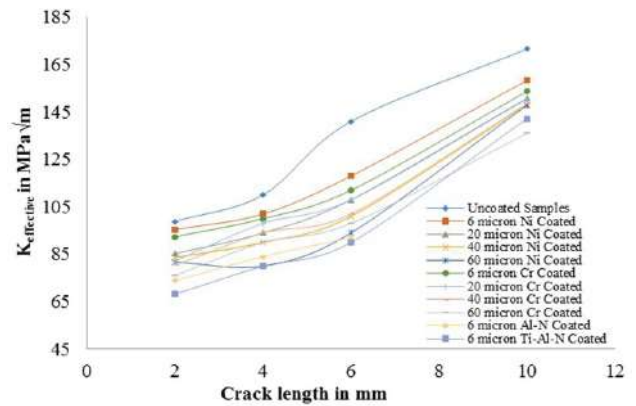

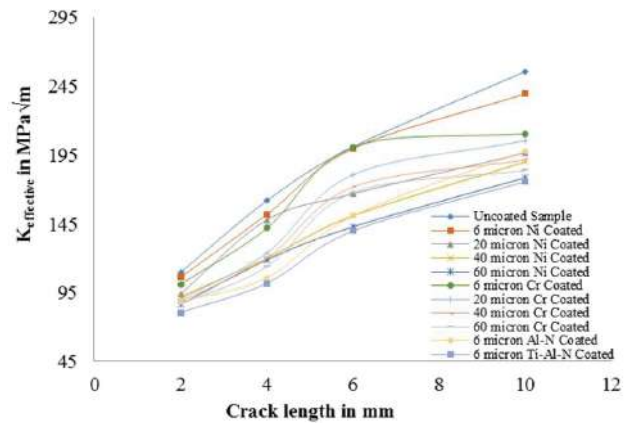**Figure 14.** $K_{effective}$ against crack length for one year pitting corroded steel samples

Figure 15. $K_{effective}$ against crack length for five year pitting corroded steel samples
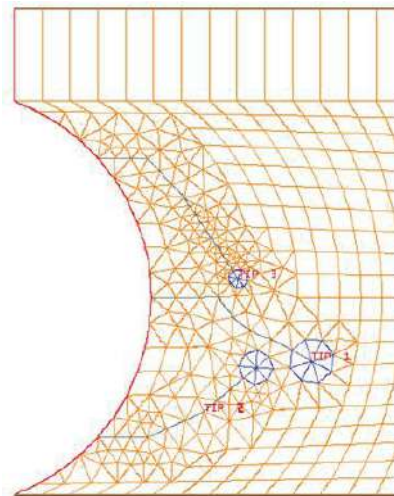

Figure 16. Crack growth for uniformly and pitting corroded samples.

The pitting and uniform corrosion are combined, and simulation was carried shown in figure 16 and figure 17. As per figure 16, when the multiple cracks were grown,
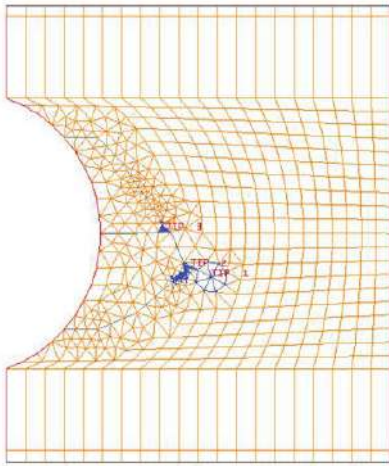
Figure 17. Crossing of one crack on the other

two or three cracks are seen to be meeting. It is observed in figure 17 that the two cracks followed upon their meeting, lead to chipping of part of the substrate and leading to failure of the entire structural component.

In figure 18, the combination of pitting and uniform corrosion together increased the $K_{effective}$ values compared to the total effect of uniform and pitting corrosion separately. The same phenomenon of PVD and higher coating thickness samples show a linear behavior in $K_{effective}$ values with increase in crack length. Other samples showed a nonlinear behavior as shown in figure 18.
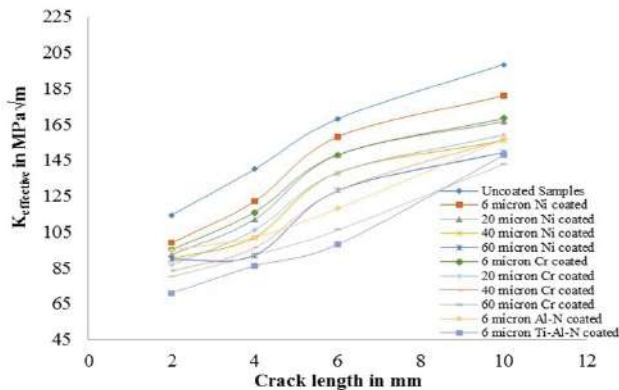
Figure 18. $K_{effective}$ against crack length for one year pitting and uniformly corroded steel samples

Increase in corrosion rate leads to more reduction in thickness of samples in combined corrosion phenomenon from figure 19. A rise in $K_{effective}$ values can be found because of the combined corrosion phenomenon. The PVD and higher coating thickness samples showed almost nonlinear behavior. In case of other coated samples showed a highly nonlinear behavior at 6mm crack length and 10mm crack length. The kinking of crack is drastic with a reduction in thickness, and $K_{effective}$ values are affected, and the

same is illustrated using figure 19.

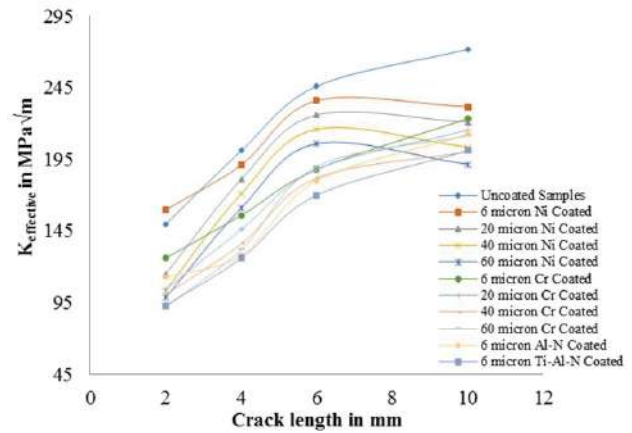**Figure 19.** $K_{effective}$ against crack length for five year pitting and uniformly corroded steel samples

In the case of electroplated aluminum samples, the behavior of $K_{effective}$ values was different from figure 20. Compared to uncoated and higher coating thickness samples the 6μ Ni coated samples showed increased $K_{effective}$ values because of reduction in thickness. The coated samples showed a linear behavior compared to uncoated cases which are showing highly nonlinear and is as observed in figure 20.
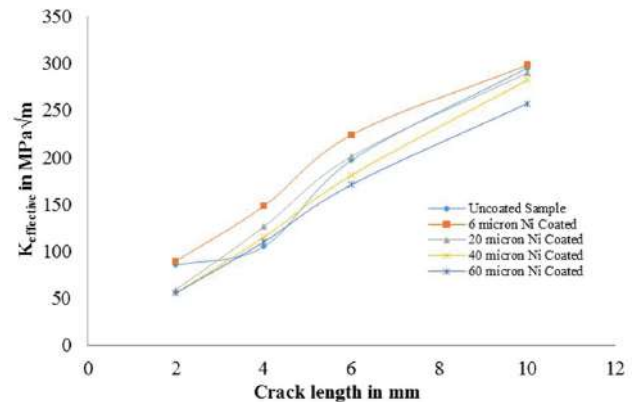

Figure 20. $K_{effective}$ against crack length for one year uniformly corroded aluminum samples

Further increase in corrosion rate result increased the $K_{effective}$ values as per figure 21. The uncoated samples showed a highly nonlinear behavior with a drastic increase in $K_{effective}$ values with increase in crack length. Other samples showed almost a linear behavior except 6μ Ni coated samples showed high $K_{effective}$ values.

As for the pitting corrosion of aluminum coated samples, there is increase in corrosion resistance due to the increase in coating thickness. It is shown in figure 22. All the coated and uncoated samples showed a drastic in-

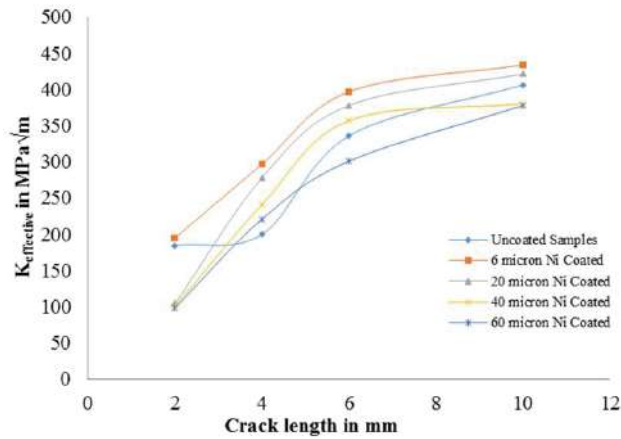crease $K_{effective}$ values with increase in crack length.

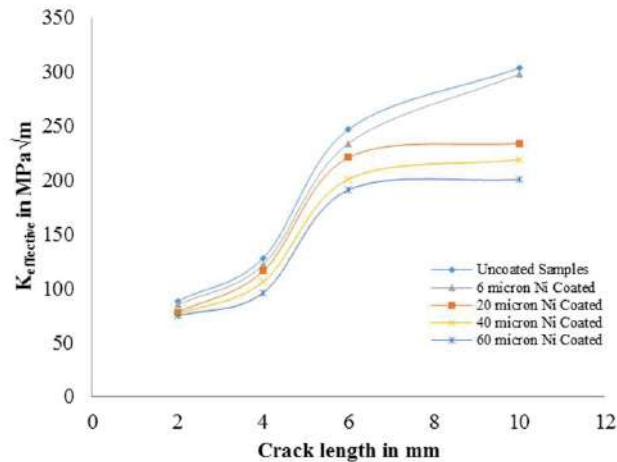**Figure 21.** $K_{effective}$ against crack length for five year uniformly corroded aluminum samples

Figure 22. $K_{effective}$ against crack length for one year pitting corroded aluminum samples

Figure 23 shows that an increase in corrosion rate will raisethe the Keffective values. A sudden rise in $K_{effective}$ values can be observed in figure 23 near or around a crack length of 6mm. When the pit depth is increased, and stress around are also increased and with the introduction of crack the $K_{effective}$ values are shooting up as per figure 23.

In the combined case of pitting and uniform corrosion, the case of 6μ Ni coated samples showed an increase in $K_{effective}$ values and i8s shown in figure 24. Compared to pitting corrosion the uniform corrosion is dominating in corrosion rate by causing the reduction in thickness.

Therefore, compared to other samples the 6μ Ni coated samples shows a increased $K_{effective}$ values along with an increase in corrosion rate.

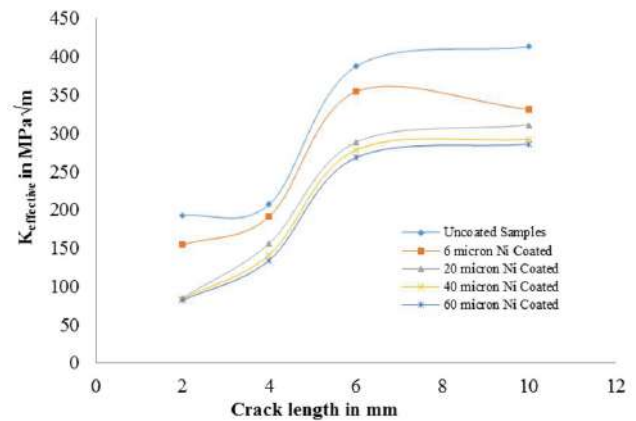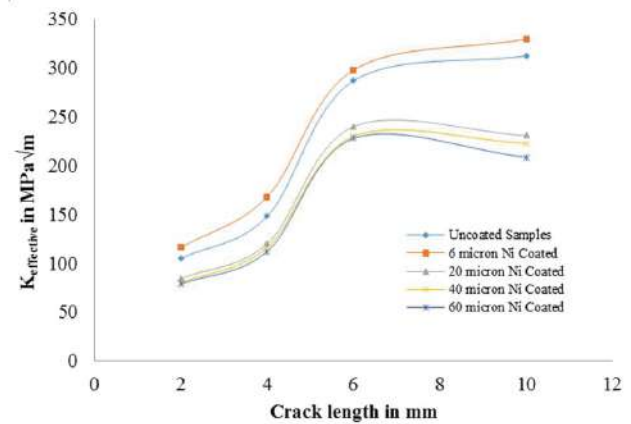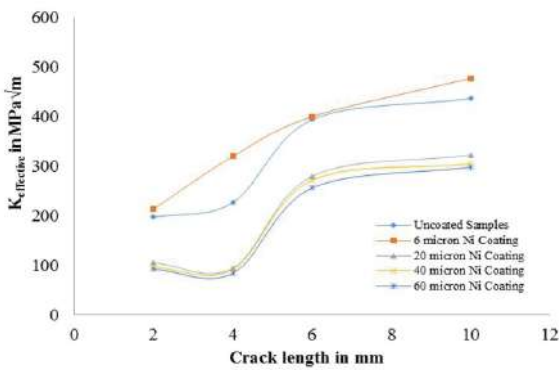**Figure 23.** $K_{effective}$ against crack length for five year pitting corroded aluminum samples

Figure 24. $K_{effective}$ against crack length for one year pitting and uniformly corroded aluminum samples

Figure 25 shows an increase in corrosion rate triggering a drastic increase in $K_{effective}$ values. The 6μ Ni coated samples showed a linear increase of $K_{effective}$ values with increase crack length. The uncoated samples and higher coating thickness samples showed a nonlinear behavior at 4mm and 6mm crack length. The pitting depth is influencing the behavior at a certain crack lengths and is shown in figure 25.

Fatigue analysis was performed for estimating the number of cycles against corrosion years for coated and uncoated samples of steel and aluminum. The analysis was performed by considering the effects of uniform, pitting and uniform and pitting together through figures 26-31. Figure 26 shows a number of cycles for different coated components, from the figure the uncoated samples shows a less number of cycles. The increase in coating thickness increased the corrosion resistance and increased the number of cycles.

Figure 25. $K_{effective}$ against crack length for five years pitting and uniformly corroded aluminum samples
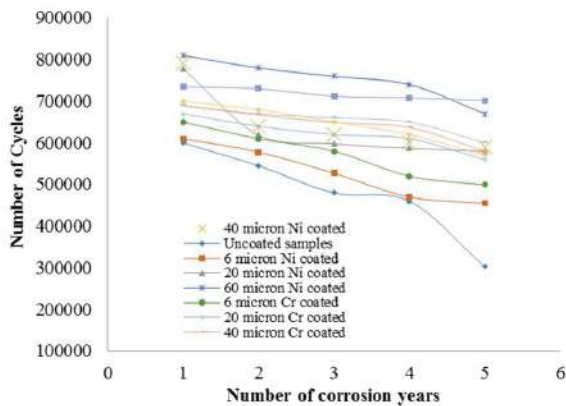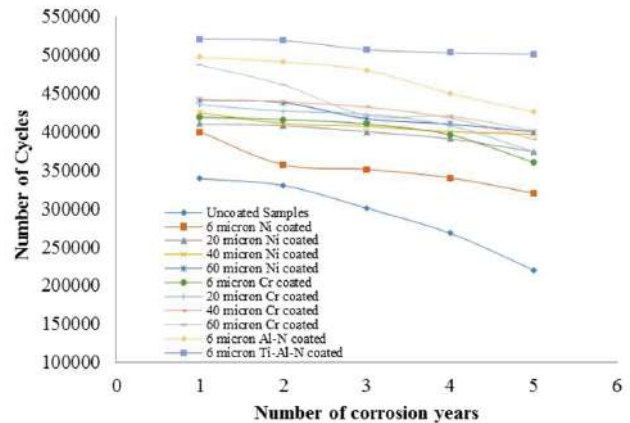

Figure 26. Number of cycles against corrosion years for uniformly corroded steel samples

In pitting corrosion even though the uncoated samples showed less number of cycles, other coated samples showed a different behaviors. The number cycles decreased with increase in corrosion years, but 6µ and 60µ Ni coated samples showed a different behavior with increasing the number of cycles at certain and then reducing as per figure 27.
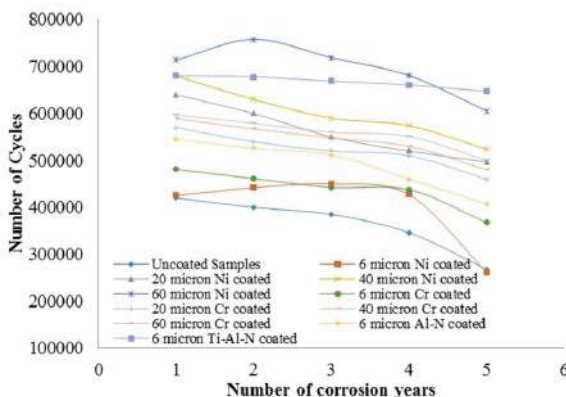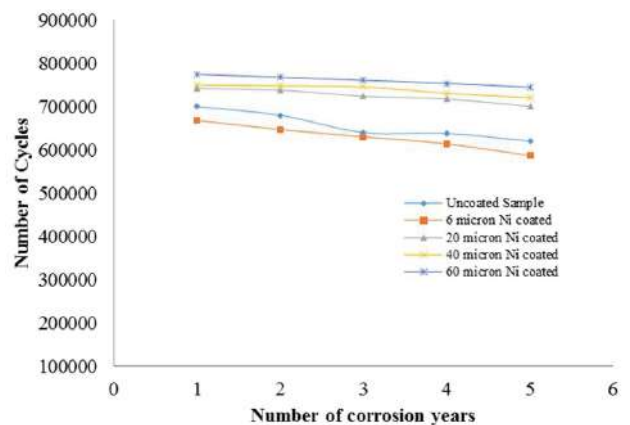

Figure 27. Number of cycles against corrosion years for pitting corroded steel samples

In figure 28 the combined corrosion phenomenon showed a decreased number of cycles with the increase in corrosion years. The 60µ Cr coated samples showed a reduction in a number of cycles for a three year duration of corrosion. Although increase in coating thickness increases the corrosion resistance, there is a decrease in the coating toughness and the number of cycles.
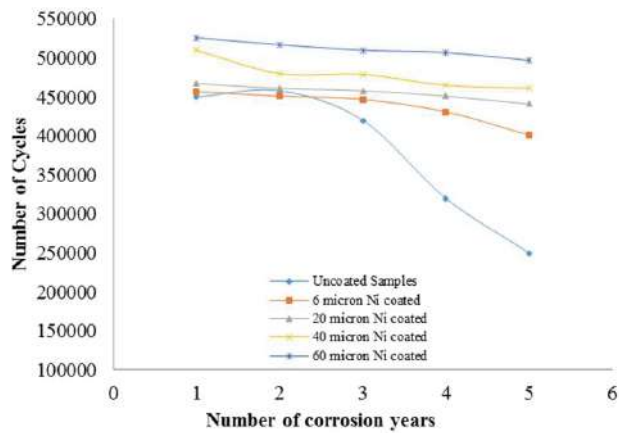

Figure 28. Number of cycles against corrosion years for pitting and uniformly corroded steel samples

For aluminium coated samples, there is increase in a number of cycles for an increase in coating thickness except for 6µ Ni coated samples as per figure 29. The increase in corrosion rate on the 6µ Ni coated samples result in reducing the number of cycles.
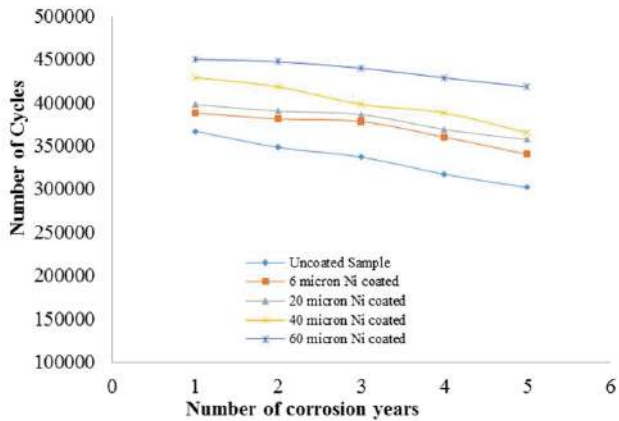

Figure 29. Number of cycles against corrosion years for uniformly corroded aluminium samples

In the case of pitting corrosion of aluminum samples, the uncoated sample showed an increase in a number of cycles and again decreased from figure 30. The pit depth is effecting the performance of the crack, and the number of cycles is found diminished.

31

Figure 30. Number of cycles against corrosion years for pitting corroded steel samples

The combined effect of corrosion on aluminum coated samples did not affect much on coated samples as per figure 31. The increase in coating thickness increased the corrosion resistance and increased the number of cycles.


Figure 31. Number of cycles against corrosion years for pitting and uniformly corroded aluminum samples

The elevation of coating thickness is important for the improvement of performance of structures in severe marine environment. The most important property is toughness of coating in different conditions. For measuring this, an indentation testing is carried out for a different range of loads varying in steps of 10N, 50N, 200N, 500N and 1250 at room temperature for corroded and uncorroded samples. The SEM analysis is done for all coated sample and fracture toughness of all coating is compared. Equation (4) is used for determining the fracture toughness and found that PVD coated samples of Al-N and Ti-Al-N samples showed better fracture toughness values compared to electroplated samples. Later the uncorroded and corroded samples were compared for analysis. In figure 32 the

uncorroded Ni-coated steel sample showed more cracks compared to Cr coated samples.
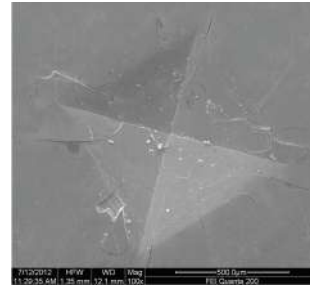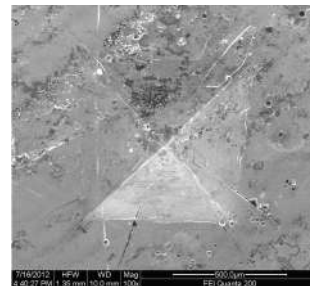

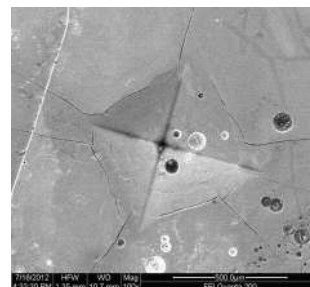**Figure 32.** SEM image of uncorroded Ni-coated steel samples
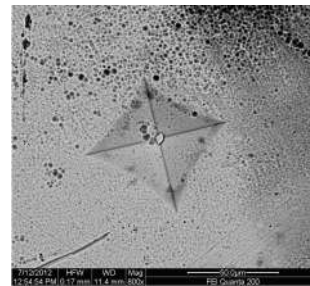
Figure 33. SEM image of corroded Ti-Al-N coated steel samples
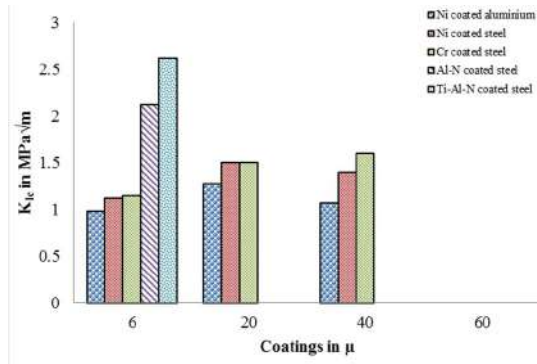
The Ti-Al-N samples from figure 33 showed no cracks which indirectly increased the fracture toughness of the coating.

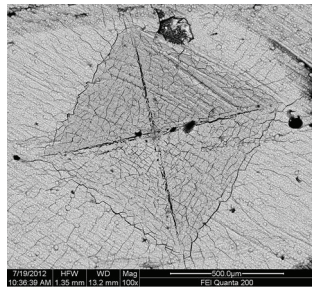**Figure 34.** SEM image of corroded Ni-coated steel samples

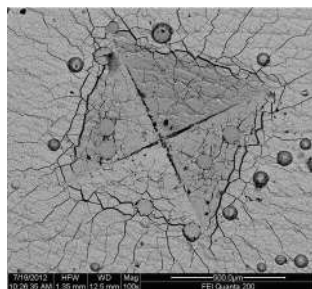**Figure 35.** SEM image of corroded Cr coated steel samples

Figure 36. K_{Ic} against coating thickness for uncorroded steel and aluminum

Later the indentation near the pitting was conducted and found that a decrease in fracture toughness with an increase of some cracks. It is shown in figure 36. The increase in some cracks was due to micro pits formed around the main pitted area. Comparatively, Cr coated samples showed less number of cracks due to an increase in corrosion resistance as per figure 37.

Though the increase in coating thickness is decreasing the rate of corrosion, it is affecting the fracture toughness of the coating. Due to the increase in coating thickness, the residual stress is increased and is seen from figure 38. This phenomena indirectly affects the coating toughness with multiple cracks. Similar behavior can be observed in 60μ Ni coated aluminum samples. Figure 38 shows the chipping of the coating due to poor adherence.

Figure 37. SEM image of corroded 60μ Cr coated steel samples

Figure 38. SEM image of corroded 60μ Ni coated aluminum samples
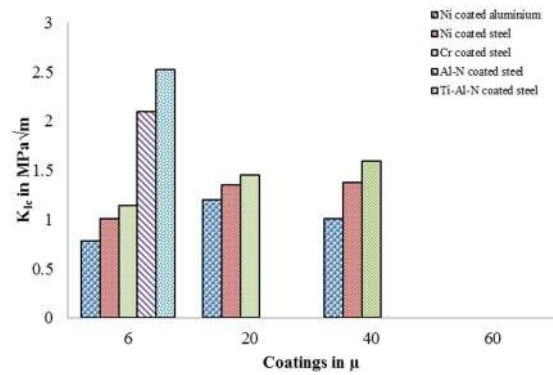
Figure 39. K_{Ic} against coating thickness for uncorroded steel and aluminum

Figure 39 shows higher fracture toughness values are seen for PVD coated samples compared to electroplated Ni and Cr samples.

5. Conclusion

In the present study, the samples of high strength steel were coated with different coating methods like electroplating of Ni and Cr and PVD coating by Al-N and nano crystalline Ti-Al-N. The aluminum samples were coated with electroplating of Ni. All samples of steel and aluminium were tested by potentiodynamic polarization by ASTM G-59 and weight loss test by ASTM G-39. Following were concluded

※ Pitting and uniform corrosion on high strength steel showed that PVD coated nano crystalline Ti-Al-N and Al-N coated samples showed an excellent corrosion resistance property compared to Ni and Cr electroplated samples. 6μ of PVD coated samples showed good results compared to 20μ, 40μ and 60μ electroplated samples. Therefore, the method of coating along with coating thickness affects the performance of structural materials.

※ In pitting corrosion of Ni-coated aluminum samples increase with coating thickness. It means an increase in corrosion resistance. But in uniform corrosion due to deposition of salt on the surface of Ni-coated aluminum decreases the corrosion resistance.

※ $K_{effective}$ values are found very high for combined corrosion rate of uniform and pitting, compared to individual pitting and uniform corrosion rate.

※ Growing of multiple cracks near the corroded area showed a possibility of the crossing of cracks. Such phenomena are demonstrated using simulation.

※ Fatigue crack growth analysis showed the decrease in a number of cycles for combined corrosion rate of uniform and pitting, compared to individual pitting and uniform corrosion rate. The coating thickness and methods of coating affected the fatigue crack growth life of the samples.

　※ Indentation tests showed that PVD coated samples were better in fracture toughness than electroplated samples. This is relevant for both cases of before and after corrosion.

Author Contributions

It is the PhD work of the first author. He is strong in experimental works and has good exposure to numerical and computer simulations. The second author is the research guide of Dr Manjunath.

References

[1] P. V. Petroyiannis, Al. Th. Kermanidis, P. Papanikos, Sp. G. Pantelakis, Corrosion-induced hydrogen embrittlement of 2024 and 6013 aluminum alloys, Theoretical and Applied Fracture Mechanics, 2004, 41, 173–183.

[2] Sp. G. Pantelakis, P. G. Maglaras, Ch. Alk. Apostolopoulos, Tensile and energy density properties of 2024, 6013, 8090 and 2091 aircraft aluminum alloy after corrosion exposure, Theoretical and Applied Fracture Mechanics, 2000, 33, 117-134.

[3] D. Birchon, The use and abuse of materials in ocean engineering, Proceedings of the Institution of Mechanical Engineers,1970, 24, 185.

[4] D. G. Harlow and R. P. Wei, A probability model for the growth of corrosion pits in aluminum alloy induced by constituent particles, Engineering Fracture Mechanics,1998, 59, 305-325.

[5] M Ramana Pidaparti, S. Appajoysula Rao, Analysis of pits induced stresses due to metal corrosion, Corrosion Science, 2008, 50, 1932-1938.

[6] T. G. Gooch and G. S. Booth, Corrosion fatigue of offshore structures, Metal Science,1979, 402-410.

[7] S. P. Lynch, Failures of structures and components by environmentally assisted cracking, Engineering Failure Analysis, 1994, 1(2), 77-90.

[8] Torgeir Moan, Efren Ayala-Uraga, Reliability-based assessment of deteriorating ship structures operating in multiple sea loading climates, Reliability Engineering and System Safety, 2008, 93, 433-446.

[9] Franc2d Users manual. www.cfg.cornell.edu.

[10] A. Dale Cope, S. Patrick Johnson, Angela Trego, and J. Doug West, Analytical framework for the assessment of corrosion and fatigue in fuselage lap joint, (1998) Boeing Information, Space and Defence systems, Wichita, Kansas 627277 USA. http://tregoengineering.com/PDF_Papers/afcp1998_anal_meth_dadT.pdf

[11] P. Richard Gangloff. Environmental cracking - corrosion fatigue. http://www.virginia.edu/ms/faculty/gangloffASTM

[12] Domenico "Nico" Quaranta, FRANC2D/L crack growth users guide, 2011, Revision 1.5.5.

[13] ASTM G-59 standard test method for conducting potentiodynamic polarization resistance measurements.

[14] ASTM G-31 Standard Practice for laboratory immersion corrosion testing of metals.

[15] J. Lesage, A. Roman, and D. Chicot. Indentation tests determine the fracture toughness of nickel-phosphorus coatings. Surface and Coatings Technology , 2002, 5, 161-168.

[16] B. Zaid, D. Saidi, A. Benzaid, S. Hadji. Effects of pH and chloride concentration on pitting corrosion of AA6061aluminum alloy. Corrosion Science, 2008, 50, 1841–1847.

[17] Hiroki Tamura, The role of rusts in corrosion and corrosion protection of iron and steel, Corrosion Science, 2008, 50,1872-1883.

[18] Ramana M. Pidaparti, Babak Seyed Aghazadeh, Angela Whitfield, A. S. Rao and Gerald P. Mercier. Classification of corrosion defects in Ni-Al bronze through image analysis. Corrosion Science, 2010, 52, 3661-3666.

[19] Allachi. H, Chaouket. F, Draoui. K. Protection against corrosion in marine environments of AA6060 aluminum alloy by cerium chlorides. Journal of Alloys and Compounds, 2010, 491, 223-229.

[20] Park Y I. Time-dependent risk assessment of aging ships. A Doctoral thesis submitted to Pusan State University on February 2004.

[21] Paik J K and Kim D K. Advanced method for the development of an empirical model to predict time-dependent corrosion wastage. Corrosion Science, 2012, 63, 51–58.

[22] Mohd Hairil Mohd, Do Kyun Kim, Dong Woo Kim, and Jeom Kee Paik. A time-variant corrosion wastage model for subsea gas pipelines. Available online from 18 March 2013.

[22] Manjunath G L and Surendran S. Effect of mono and composite coating on dynamic fracture toughness of metals at different temperatures. Composite Part B. Accepted on 11/03/2013.